[6] K. Ise and M. Koshiba, "Numerical analysis of H-plane waveguide junctions by combination of the finite and boundary elements," *IEEE Trans. Microwave Theory Tech.*, vol. 36, pp. 1343–1351, Sept. 1988.
[7] J. M. Reiter and F. Arndt, "Rigorous analysis of arbitrarily shaped H- and E-plane discontinuities in rectangular waveguides by a full-wave boundary contour mode-matching method," *IEEE Trans. Microwave Theory Tech.*, vol. 43, pp. 796–801, Apr. 1995.
[8] A. M. Khilla and I. Wolff, "Field theory treatment of H-plane waveguide junction with triangular ferrite post," *IEEE Trans. Microwave Theory Tech.*, vol. MTT-26, pp. 279–287, Apr. 1978.
[9] F. Arndt, R. Beyer, J. Reiter, T. Sieverding, and T. Wolf, "Automated design of waveguide components using hybrid mode-matching/numerical em building-blocks in optimization-oriented CAD frame-works—State-of-the-art and recent advances," *IEEE Trans. Microwave Theory Tech.*, vol. 45, pp. 747–760, May 1997.
[10] F. Alessandri, G. Bartolucci, and R. Sorrentino, "Admittance matrix formulation of waveguide discontinuity problems: Computer-aided design of branch guide directional couplers," *IEEE Trans. Microwave Theory Tech.*, vol. 36, pp. 394–403, Feb. 1988.
[11] R. H. MacPhie and K.-L. Wu, "A full wave modal analysis of arbitrarily shaped waveguide discontinuities using the finite plane-wave series expansion," *IEEE Trans. Microwave Theory Tech.*, vol. 47, pp. 232–237, Feb. 1999.
[12] M. Guglielmi, "Simple CAD procedure for microwave filters and multiplexers," *IEEE Trans. Microwave Theory Tech.*, vol. 42, pp. 1347–1352, July 1994.
[13] V. E. Boria, M. Guglielmi, and P. Arcioni, "Computer-aided design of inductively coupled rectangular waveguide filters including tuning elements," *Int. J. RF Microwaves Computer-Aided Eng.*, vol. 8, pp. 226–236, May 1998.
[14] A. Alvarez, G. Connor, and M. Guglielmi, "New simple procedure for the computation of the multimode admittance or impedance matrix of planar waveguide junctions," *IEEE Trans. Microwave Theory Tech.*, vol. 44, no. 3, pp. 413–418, March 1996.
[15] H. Patzelt and F. Arndt, "Double-plane steps in rectangular waveguides and their application for transformers, irises, and filters," *IEEE Trans. Microwave Theory Tech.*, vol. MTT-30, pp. 771–776, May 1982.
[16] M. Koshiba and M. Suzuki, "Finite-element analysis of H-plane waveguide junction with arbitrarily shaped ferrite post," *IEEE Trans. Microwave Theory Tech.*, vol. 34, pp. 103–109, Jan. 1986.
[17] J. P. Webb and S. Porihar, "Finite element analysis of H-plane rectangular waveguide problems," *Proc. Inst. Elect. Eng.*, vol. 133, pp. 91–94, Apr. 1986.
[18] A. Taflove, *Computational Electromagnetics: The Finite-Difference Time-Domain Method*. Norwood, MA: Artech House, 1995.
[19] Y. Leviatan and G. S. Sheaffer, "Analysis of inductive dielectric posts in rectangular waveguide," *IEEE Trans. Microwave Theory Tech.*, vol. MTT-35, pp. 48–59, Jan. 1987.
[20] G. S. Sheaffer and Y. Leviatan, "Composite inductive posts in waveguide—A multifilament analysis," *IEEE Trans. Microwave Theory Tech.*, vol. 36, pp. 779–783, Apr. 1988.
[21] A. Valero and M. Ferrando, "Full-wave equivalent network representation for multiple arbitrarily shaped posts in H-plane waveguide," *IEEE Trans. Microwave Theory Tech.*, vol. 47, pp. 1997–2002, Oct. 1999.
[22] A. Boetteger, T. Sieverding, P. Krauss, and F. Arndt, "Fast boundary contour mode-matching method for the CAD of circular post coupled resonator filters," in *Proc. 28th Eur. Microwave Conf.*, Oct. 1998, pp. 712–715.
[23] C. A. Balanis, *Advanced Engineering Electromagnetics*. New York: Wiley, 1989.
[24] H. Esteban, V. E. Boria, M. Baquero, and M. Ferrando, "Generalized iterative method for solving 2D multiscattering problems using spectral techniques," *Proc. Inst. Elect. Eng.*, pt. H, vol. 144, no. 2, pp. 73–80, Apr. 1997.
[25] N. Marcuvitz, *Waveguide Handbook*, ser. Electromag. Wave 21. London, U.K.: IEE Press, 1986.
[26] J. Abdulnour and L. Marchildon, "Boundary elements and analytic expansions applied to H-plane waveguide junctions," *IEEE Trans. Microwave Theory Tech.*, vol. 42, pp. 1038–1045, June 1994.
[27] C.-I. Hsu and A. Auda, "Multiple dielectric posts in a rectangular waveguide," *IEEE Trans. Microwave Theory Tech.*, vol. MTT-34, pp. 883–891, Aug. 1986.
[28] A. Weisshaar, S. M. Goodnick, and V. K. Tripathi, "A rigorous and efficient method of moments solution for curved waveguide bends," *IEEE Trans. Microwave Theory Tech.*, vol. 40, pp. 2200–2206, Dec. 1992.

A Balanced FET FMCW Radar Transceiver With Improved AM Noise Performance

Christian Fager, Klas Yhland, and Herbert Zirath

***Abstract*—A balanced FET frequency-modulated continuous-wave radar transceiver designed to suppress AM noise is presented. The transceiver utilizes the same device for output power amplification as for down-conversion of the received signal, thereby avoiding the need for separation of these signals. This makes the transceiver suitable for integration in monolithic-microwave integrated-circuit technology. A test circuit operating at 10 GHz was designed. The AM noise suppression is characterized, as well as output power and noise performance. Comparison with an unbalanced transceiver using the same principle of operation shows an improvement of 20 dB in AM noise performance. The output power is 14 dBm at 7-dBm input power.**

***Index Terms*—AM noise, FMCW, radar, transceiver.**

I. Introduction

The use of frequency-modulated continuous-wave (FMCW) radars for different high-volume applications, such as automotive collision avoidance, cruise control, and fluid-level indicators has increased in recent years. Several approaches to the design of the transceivers used for those radars have been presented [1]–[3].

Recently, the authors presented a novel FET transceiver suitable for FMCW radar applications [4]. The transceiver utilizes a single FET to simultaneously amplify the transmitted signal, and as a resistive mixer, to down-convert the received signal, making it suitable for integration in monolithic-microwave integrated-circuit (MMIC) technology.

One major limitation of the performance of FMCW radars comes from noise in the transmitter oscillator being down-converted to baseband in the receiver. This can limit the dynamic range of the radar and, thus, decrease the resolution.

AM noise from the transmitter oscillator can significantly contribute to the IF noise in the receiver [5], and should, if possible, be suppressed. Different methods to suppress AM noise in FMCW transceivers have been reported [6], [7]. Most of them utilize balanced topologies.

For short-range radars, the received and transmitted signals are strongly correlated. In most short-range FMCW radars, the same oscillator is used for the transmitter and receiver mixer. The oscillator FM noise will then cancel in the down-conversion of the received signal [5], [6]. For short-range radars, AM noise is, therefore, generally more severe than FM noise.

In this paper, we present a balanced design of the unbalanced FET transceiver [4] with improved capability of AM noise suppression in FMCW radar applications.

II. Balanced Circuit Topology

When analyzing the FET transceiver, it can be considered as a FET resistive mixer with the input signal (IN) serving as a local oscillator (LO) and the LO to RF leakage providing the transmitted signal

Manuscript received March 4, 2001.

C. Fager and K. Yhland are with the Microwave Electronics Laboratory, Department of Microelectronics, Chalmers University of Technology, SE-412 96 Göteborg, Sweden (e-mail: fager@ep.chalmers.se).

H. Zirath is with the Microwave Electronics Laboratory, Department of Microelectronics, Chalmers University of Technology, SE-412 96 Göteborg, Sweden and also with Ericsson Microwave Systems AB, SE-431 84 Mölndal, Sweden.

Publisher Item Identifier S 0018-9480(02)03023-5.

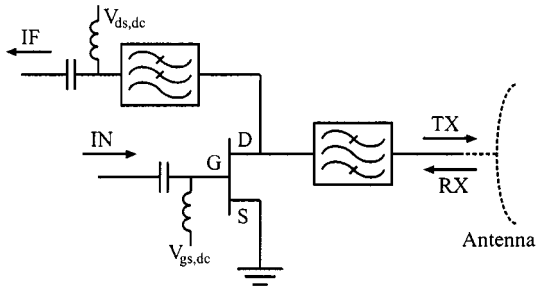

Fig. 1. Circuit diagram of the unbalanced FET transceiver.

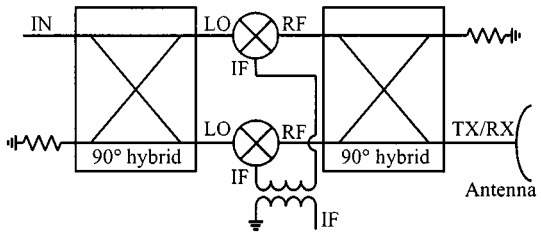

Fig. 2. Balanced FET transceiver topology.

(Fig. 1). As opposed to most other mixer applications, the LO to RF leakage should, therefore, be maximized.

To prevent down-conversion of the AM noise of the IN signal to the IF, a balanced topology is investigated. For this application, a singly balanced quadrature hybrid configuration, which is shown in Fig. 2, is suitable.

This configuration has good LO AM noise rejection properties and low LO to RF port isolation [7]. Furthermore, the ports will be well matched.

III. Circuit Design

A balanced circuit at 10 GHz was realized in microstrip technology on a 0.38-mm-thick Duroid 5870 substrate. The circuit was built without tuning at any frequencies.

Two NEC NE 32400 chip FETs from the same batch as used in the unbalanced FET transceiver [4] were used. The layout of the balanced test circuit is shown in Fig. 3.

The circuit was designed to make each FET unconditionally stable. The stabilization was implemented using one 10-Ω series and one 100-Ω shunt resistor at each gate.

The 90° hybrids were designed as double-section branchline couplers, having a bandwidth of approximately 3 GHz. For the IF balun, a Mini-Circuits T4-6T surface-mount RF transformer was used, with 3 dB operating frequency range from 20 kHz to 250 MHz. The transformer impedance ratio is 4 : 1, which makes the IF impedance 100 Ω, as seen from each FET. The center tap of the transformer was used for drain dc biasing.

IV. Measured Performance

To evaluate the performance of the balanced transceiver, it is compared with the unbalanced FET transceiver [4].

The IN power (P_{IN}) used for the balanced circuit was 7 dBm, which is 4 dB higher than used in the unbalanced configuration. This compensates for power division in the input coupler and losses in the stabilizing resistors.

A. Output Power and Conversion Loss

The output power (P_{TX}) and conversion loss (CL) were measured versus gate dc bias voltage ($V_{\mathrm{gs,dc}}$) and drain dc bias voltage ($V_{\mathrm{ds,dc}}$) using the same setup described in [4]. The IN- and RX frequencies were 10.01 and 10 GHz, respectively.

Using $P_{\mathrm{TX}}/\mathrm{CL}$ as a figure-of-merit, the optimum bias was found to be $V_{\mathrm{gs,dc}} = -0.4$ V and $V_{\mathrm{ds,dc}} = 2.0$ V. With this bias, P_{TX} and CL were found to be 14.0 dBm and 8.6 dB, respectively, for the balanced transceiver. Fig. 4 shows how P_{TX}, CL, and $P_{\mathrm{TX}}/\mathrm{CL}$ vary versus P_{IN} at the optimum bias point.

Compared with the unbalanced transceiver [4], P_{TX} is approximately 3.5 dB higher, and $P_{\mathrm{TX}}/\mathrm{CL}$ improved by 4 dB for the balanced circuit at $P_{\mathrm{IN}} = 3$ dBm. Similar to the unbalanced transceiver, the $P_{\mathrm{TX}}/\mathrm{CL}$ optimum is found to be insensitive to bias variations. $P_{\mathrm{TX}}/\mathrm{CL}$ varies less than 3 dB for $V_{\mathrm{ds,dc}}$ ranging from 1.3 to 2.5 V, and $V_{\mathrm{gs,dc}}$ ranging from -0.8 to -0.2 V. The optimum bias differs from the unbalanced circuit due to different embedding impedances.

B. Double-Sideband Noise Power Density at the RX/TX Port

Using the same procedure as described in [4], the double-sideband noise power density referred to the RX/TX port (P_{DSB}) was measured versus f_{IF} at $f_{\mathrm{IN}} = 10.5$ GHz. The result is shown in Fig. 5.

Compared to the unbalanced design, P_{DSB} is somewhat lower for the balanced transceiver at low frequencies. This is caused by the limited bandwidth of the IF transformer.

Since in Fig. 5 no significant improvement in the noise performance is seen between the two transceivers, the main contribution to the noise in this setup is probably from FM noise in the signal generator and $1/f$ noise from the FETs.

C. AM Noise Suppression

To study how AM sidebands of the IN signal are converted to IF, the IN signal was amplitude modulated. The IN signal sideband levels were adjusted to be approximately 25 dB below the IN signal level, which corresponds to a modulation index $m = 11\%$.

The AM noise suppression is proportional to the ratio between the down-converted AM signal level at the IF port ($P_{\mathrm{IF,AM}}$) and m^2. Since the desired IF signal level is proportional to $P_{\mathrm{TX}}/\mathrm{CL}$, an AM demodulation sensitivity S_{AM} can be defined as follows:

$$S_{\mathrm{AM}} = \frac{\dfrac{P_{\mathrm{TX}}}{\mathrm{CL}}}{\dfrac{P_{\mathrm{IF,AM}}}{m^2}}. \tag{1}$$

$P_{\mathrm{TX}}/\mathrm{CL}$ is measured using the same procedure as in [4]. The power at the IF port was measured using an HP 8565E spectrum analyzer. During the AM measurements, the RX/TX port was terminated in a 50-Ω load.

Fig. 6 compares S_{AM} of the balanced and the unbalanced transceivers for a swept IN frequency (f_{IN}) at $f_{\mathrm{IF}} = 10$ kHz. The circuits were biased at their respective optimum $P_{\mathrm{TX}}/\mathrm{CL}$ bias voltages.

In the balanced circuit, the suppression is substantially improved (Fig. 6). The variation of S_{AM} for the balanced transceiver, seen in Fig. 6, corresponds closely to the simulated amplitude balance of the input branchline coupler. The AM suppression is determined by the amplitude balance of the input branchline coupler and the amplitude and phase balance of the IF transformer. We believe it is realistic to improve the AM noise suppression of the balanced circuit compared to the unbalanced circuit by 20 dB all over the measured bandwidth by optimizing the amplitude balance of the input coupler since this was not originally done.

Fig. 7 shows S_{AM} versus f_{IF} for the balanced and unbalanced transceivers at $f_{\mathrm{IN}} = 10.5$ GHz. For $f_{\mathrm{IF}} < 500$ kHz, where the impact of

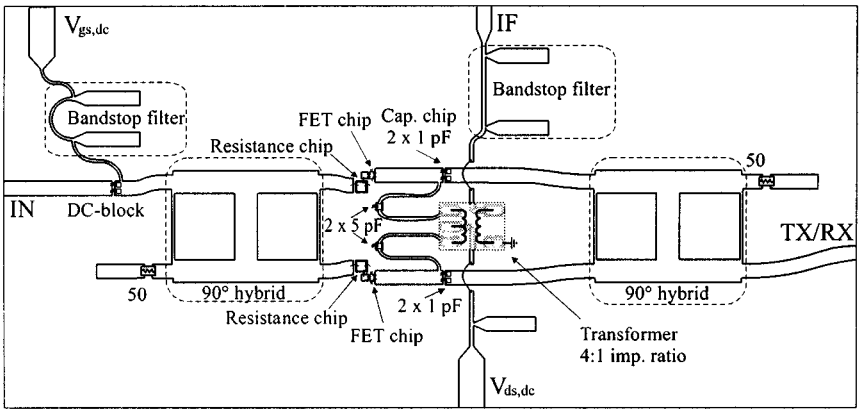

Fig. 3. Layout of the balanced FET transceiver test circuit.

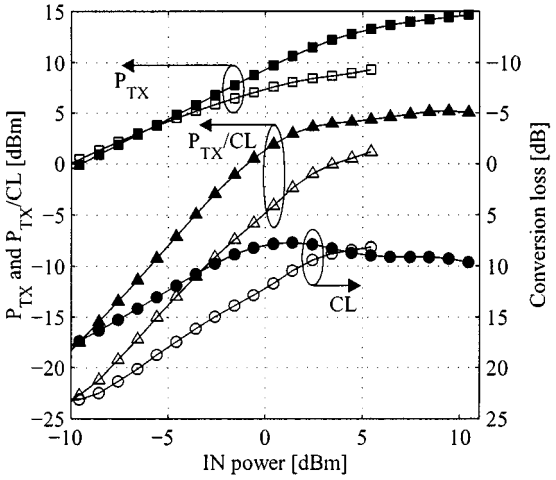

Fig. 4. Measured transmitted power ($P_{\rm TX}$), conversion loss ($\rm CL$), and $P_{\rm TX}/\rm CL$ versus input power ($P_{\rm IN}$). The unbalanced (transparent markers) and balanced (filled markers) transceivers are biased at their optimum $P_{\rm TX}/\rm CL$ bias voltages. The measurement error is estimated to be within ± 1 dB.

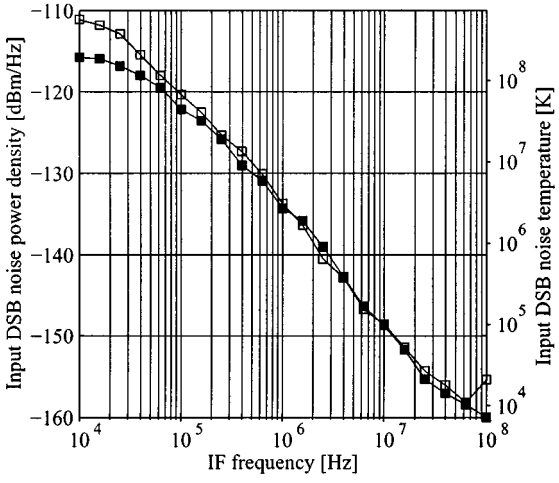

Fig. 5. Measured input DSB noise power density ($P_{\rm DSB}$) and input DSB noise temperature versus IF frequency ($f_{\rm IF}$) for the balanced (filled markers) and unbalanced (transparent markers) transceivers. The measurement error is estimated to be within ± 3 dB.

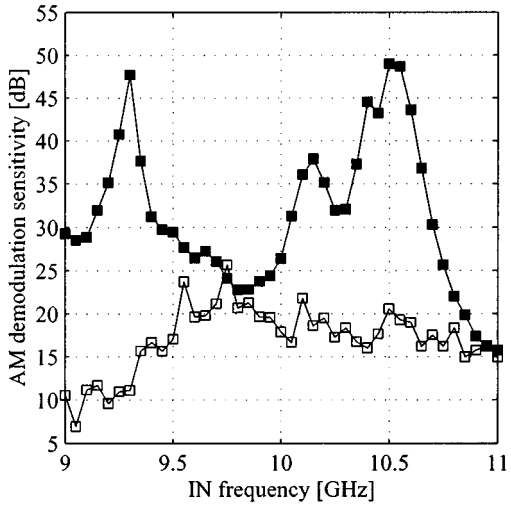

Fig. 6. Measured AM demodulation sensitivity ($S_{\rm AM}$) versus $\rm IN$ frequency ($f_{\rm IN}$) at $f_{\rm IF} = 10$ kHz for the unbalanced (transparent markers) and balanced (filled markers) transceivers. The measurement error is estimated to be within ± 3 dB.

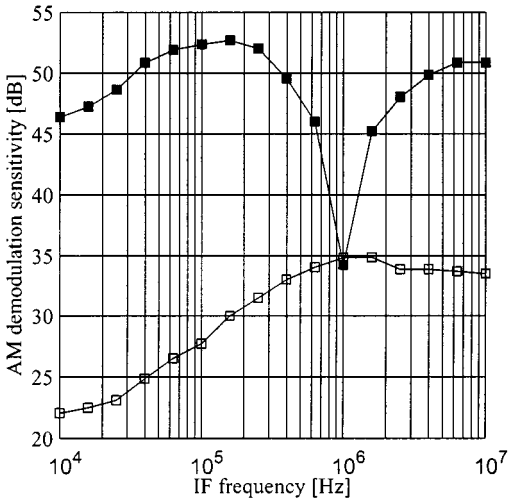

Fig. 7. Measured AM demodulation sensitivity ($S_{\rm AM}$) versus IF frequency ($f_{\rm IF}$) at $f_{\rm IN} = 10.5$ GHz for the unbalanced (transparent markers) and balanced (filled markers) transceivers.

AM noise is expected be of greatest concern, $S_{\rm AM}$ is improved by typically 20 dB for the balanced circuit compared to the unbalanced one.

A resonance is observed at $f_{\rm IF} = 1$ MHz in the balanced circuit. This is caused by the external biasing circuit.

V. Conclusions

The performance of a 10-GHz balanced FET FMCW transceiver has been investigated and compared with a similar unbalanced transceiver. The FETs in the transceiver are operated simultaneously as amplifiers and FET resistive mixers. This circumvents the need for separation between the transmitted and received signals, thus making it suitable for integration in MMIC technology.

The use of a balanced circuit topology improves the AM noise performance by typically 20 dB. The output power is 14 dBm at 7-dBm input power. Similar to the unbalanced transceiver, the balanced circuit is very robust against bias variations.

Acknowledgment

The authors thank Dr. N. Rorsman, Department of Microelectronics, Chalmers University of Technology, Göteborg, Sweden, for fruitful discussions and the reviewers for valuable comments and suggestions.

References

[1] K. W. Chang, G. S. Dow, H. Wang, T. N. Chen, K. Tan, B. Allen, I. Berenz, J. Wehling, and R. Lin, "A W-band single-chip transceiver for FMCW radar," in *Proc IEEE Microwave Millimeter-Wave Monolithic Circuits Symp.*, 1993, pp. 41–44.

[2] D. D. Si, S. C. Luo, C. Pero, W. Xiaodong, R. Knox, M. Matloubian, and E. Ponti, "Millimeter-wave FMCW/monopulse radar front-end for automotive applications," in *Proc IEEE MTT-S Int. Microwave Symp. Dig.*, 1999, pp. 277–280.

[3] J. Kehrbeck, E. Heidrich, and W. Wiesbeck, "A novel and inexpensive short range FM-CW radar design," in *Proc. Int. Radar'92 Conf.*, pp. 288–291.

[4] K. Yhland and C. Fager, "A FET transceiver suitable for FMCW radars," *IEEE Microwave Guided Wave Lett.*, vol. 10, pp. 377–379, Sept. 2000.

[5] A. G. Stove, "Linear FMCW radar techniques," *Proc. Inst. Elect. Eng.*, pt. F, vol. 139, pp. 343–50, 1992.

[6] M. I. Skolnik, *Radar Handbook*, 2 ed. New York: McGraw-Hill, 1990.

[7] S. A. Maas, *Microwave Mixers*, 2 ed. Norwood, MA: Artech House, 1993.

A Microwave Gyro Amplifier With a Ferroelectric Cathode

Moshe Einat, Eli Jerby, and Gil Rosenman

***Abstract*—A ferroelectric cathode is employed for the first time as the electron-beam source in a microwave amplifier tube. A PLZT 12/65/35 ferroelectric ceramic with a high dielectric constant ($\varepsilon_r \sim 4000$) is used in a form of a hollow cathode. The tube is operated in poor vacuum conditions (2×10^{-5} Torr) at room temperature, in a mechanism of a cyclotron-resonance maser amplifier. The device operates near the waveguide cutoff frequency at 6927 MHz. A 22-dB electronic gain and a 25-W output power are measured in this experiment.**

***Index Terms*—Cold-cathode tubes, electron emission, electron guns, ferroelectric materials, gyrotrons.**

I. Introduction

The electron gun and, more specifically, the cathode, are key elements in the design of any microwave tube [1]. In particular, cyclotron-resonance masers (CRMs) and gyro-devices can be further developed if new types of cathodes would be available. Recent records of gyro-amplifier studies, presented in [2]–[5], encourage the investigation of new types of cathodes for these devices. This paper presents a study of a ferroelectric cathode operating for the first time as an electron source for a gyro-amplifier.

The ferroelectric cathode has useful features, such as a high-density electron emission at room temperature in poor vacuum condition ($\sim 10^{-5}$ Torr). Its turn-on time is short, and it does not need any activation process. The ferroelectric cathode is easy to fabricate and it is made of low-cost materials. On the other hand, ferroelectric cathodes have a limited lifetime [6]. Studies of the electron-energy spectrum of the PLZT 12/65/35 ferroelectric cathode showed that its electron-energy spread is as large as $\sim$100 eV [7]. However, demonstrations of practical applications based on ferroelectric cathodes are still rare.

Early observations of electron emission from ferroelectrics induced by a polarization switching [8], and subsequent reports on generation of high electron current densities by ferroelectric ceramics (reaching 10^3 A/cm^2) [9], [10], stimulated development of ferroelectric cathodes by several research groups [11]–[17]. Detailed studies showed that the strong emission evolves surface flashover plasma generation, which damages the cathode surface [6], [14]–[17].

The first microwave oscillator using a ferroelectric cathode was demonstrated in our previous study [18], [19]. In the present experiment, the ferroelectric cathode serves as a hollow electron-beam source in a CRM gyro-traveling-wave tube (TWT) amplifier experiment. This CRM amplifier, operating in the fundamental gyrotron mode [20] near the cutoff frequency of the circular waveguide, tolerates the wide electron energy spread of the ferroelectric cathode. Demonstration of such a microwave amplifier may motivate the development of various low-cost devices based on ferroelectric cathodes.

II. Experimental Setup

The experimental device is shown in Fig. 1. It is comprised of an electron-gun section, a CRM interaction region, and a collector section. The electron gun is based on a ferroelectric ring cathode made on a $10 \times 10 \times 1$ mm^3 PLZT 12/65/35 ceramic plate [7]. The contact is made by silver paint at the rear (nonemitting) side of the ferroelectric plate. In the front (emitting) side, the electrode is made of a stainless-steel grid, in a ring shape of 5 and 8 mm inner and outer diameters, respectively. A metallic electrode covers the inner circle of the ring surface. The rear electrode is activated by a positive pulse of $\sim$1 kV, ~ 0.25 μs, where the front side is grounded. The first accelerating electrode is placed 5 mm in front of the cathode emitting side. This electrode, made of a stainless-steel grid, is electrically connected to the rear electrode. A dc accelerating voltage in the range of 8.5–12.5 kV is applied on the accelerating anode, at the entrance to CRM interaction region.

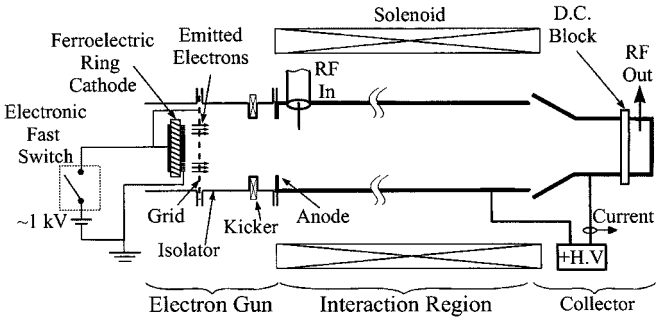

Fig. 1. Experimental gyro-amplifier device with a ferroelectric cathode.

Manuscript received May 3, 2000; revised April 30, 2001.

The authors are with the Faculty of Engineering, Tel Aviv University, Ramat Aviv 69978, Israel (e-mail: jerby@eng.tau.ac.il).

Publisher Item Identifier S 0018-9480(02)03025-9.